Identification of Vortex-Induced Clear Air Turbulence Using Airline Flight Records

E. K. Parks*
University of Arizona, Tucson, Arizona
and
R. C. Wingrove,† R. E. Bach,† and R. S. Mehta†
NASA Ames Research Center, Moffett Field, California

The nature and cause of clear-air turbulence is being investigated in cooperation with the National Transportation Safety Board, using the flight records available from airline encounters with severe turbulence. This paper presents two case studies of severe turbulence which indicate that the airplanes involved encountered vortex arrays which were generated by destabilized wind-shear layers near the tropopause. In order to identify and analyze vortex patterns (i.e., vortex strength, size, and spacings), potential-flow models of vortex arrays were developed that describe reasonably well the wind patterns derived from the airliner flight records. The results of this analysis indicate that in the two cases studied, the vortex cores had diameters in the range of 900 to 1200 ft with tangential velocities in the range of 70 to 85 ft/s. This study presents the first identification and analysis of vortex arrays from airline flight data. The results are compared with theoretical predictions and previous observations.

Nomenclature

a_x, a_y, a_z = body-axes accelerations
d = vertical separation (airplane above vortex)
g = gravitational constant
ℓ = horizontal separation (airplane beyond vortex)
Ri = Richardson number
r = perpendicular distance (vortex to airplane)
r_0 = radius of vortex core
V_a = true airspeed
V_0 = tangential velocity of vortex core
W_{xy} = horizontal wind
W_z = vertical wind
w_{xy} = vortex-induced horizontal wind
w_z = vortex-induced vertical wind
x, y, z = airplane position (Earth frame)
α = angle of attack
β = angle of sideslip, or buoyancy parameter
Γ = vortex circulation (strength)
η = two-dimensional vorticity
θ = potential temperature
ψ, θ, ϕ = body-axis Euler angles
ψ_a, γ_a = wind-axis Euler angles
$\Delta\psi$ = angle between wind vector and flightpath

Introduction

CLEAR-AIR turbulence (CAT) generally refers to turbulence in the mid to upper troposphere and in the lower stratosphere, in air that is free of clouds and strong convective currents. Most studies[1-6] indicate that severe CAT results from a breakdown of stably stratified shear layers (Kelvin-Helmholtz instability). The vortices generated by this instability soon decay into smaller vortices until the vorticity is finally dissipated by viscosity.

Encounters with severe clear-air turbulence are a continuing problem that must be better understood in the interest of airline safety. One way to investigate the nature and cause of CAT is through analysis of flight data obtained during airline encounters with severe turbulence. In the past, most flight data were obtained from the metal-foil recorders carried by narrow-body airliners. These recorders, however, do not contain enough information to permit an adequate determination of wind characteristics. Modern wide-body airliners, however, are equipped with a digital flight-data recorder that, together with ground-based air-traffic control (ATC) radar records, provides sufficient data to determine the turbulent wind environment.[7]

The present paper concerns the reconstruction and analysis of the wind environments in which two commercial airplanes encountered severe CAT. Both encounters involved wide-bodied airplanes equipped with digital flight-data recorders. The first encounter (near Hannibal, Mo., April 1981) was associated with a shear layer in the jet stream that was likely destabilized by its passage over a line of local thunderstorms. The second encounter (near Morton, Wyo., July 1982) was associated with a shear layer destabilized by waves in the lee of the Wind River Mountain range. In both of these cases, the encounters did not appear as random disturbances, such as might be associated with vortices in the later stages of dissipation, but rather as a short series of strong disturbances with a definite periodicity.

This paper examines the wind components derived from an analysis of the airline flight records. Particular emphasis is on the nature of the turbulence encountered by the airplane. Vortex modeling is used to generate winds analytically from vortex arrays arranged to match the wind components derived from the flight records. A similar technique has been used to investigate the characteristics of the trailing vortices of an airplane[8]; however, in this report vortex modeling is used to simulate the turbulence generated by Kelvin-Helmholtz shear-layer instability.

Background

Shear-Layer Instability

The tendency for a shear layer to become unstable and generate vortices is given in terms of the Richardson number

Presented as Paper 84-0270 at the AIAA 22nd Aerospace Sciences Meeting, Reno, Nev., January 9-12, 1984; received March 28, 1984; revision received July 25, 1984. This paper is declared a work of the U.S. Government and therefore is in the public domain.

*Professor of Aerospace Engineering. Associate Member AIAA.
†Aerospace Engineer. Member AIAA.

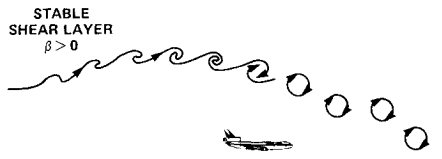

Fig. 1 Evolution of vortices in standing waves.[6]

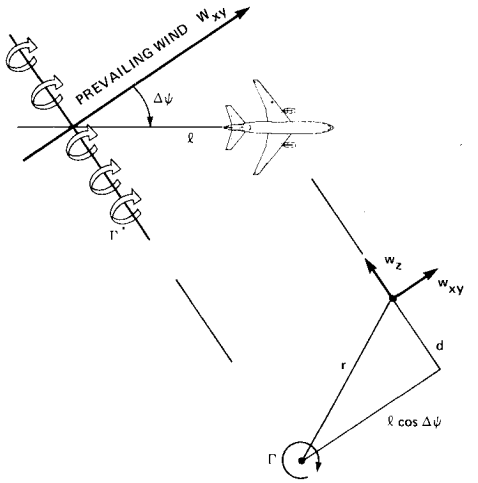

Fig. 2 Geometry used to represent the aircraft flightpath with respect to a single vortex.

(Ri $= g\beta/\eta^2$) that represents the ratio of gravity (or buoyancy) forces to the inertial (or shear) forces.[1-6] The term $g\beta$ is a restoring buoyancy force generated by the vertical displacement of a parcel of air and is a measure of static stability; η is a measure of the vorticity. For a horizontal two-dimensional shear flow, the definitions of β and η are

$$\beta = \frac{1}{\theta}\left(\frac{\partial \theta}{\partial z}\right) \quad \text{and} \quad \eta = \frac{\partial W_{xy}}{\partial z}$$

where θ is potential temperature, W_{xy} is horizontal wind speed, and z is vertical distance. It is generally accepted that a shear layer can be dynamically unstable and vortices may form when $Ri < 0.25$.

When a surface of constant potential temperature is tilted from the horizontal, a rotation of the fluid is induced to bring the surface back to the horizontal.[4,6] In the case of a two-dimensional steady flow, an incremental increase in vorticity, $\delta\eta$, occurs as[6]

$$\delta\eta = \frac{g\beta_0}{W_{xy_0}}\,\delta z \tag{1}$$

where δz is the incremental displacement from equilibrium of a parcel of air caused by tilting and where W_{xy_0}, β_0, and η_0 represent equilibrium far upstream. In this case, the Richardson number is[6]

$$Ri = \frac{g\beta}{\left(\eta_0 + \dfrac{g\beta_0}{W_{xy_0}}\,\delta z\right)^2} \tag{2}$$

It is apparent that tilting of a stable shear layer can cause a decrease in the Richardson number.

Equation (2) indicates that a large static stability (large β_0) becomes a destabilizing influence in those situations in which the streamlines are tilted.[4,6] The stability criteria discussed above are consistent with observed cases of severe CAT which often occur in statically stable layers (e.g., the isothermal layer at the tropopause, temperature inversion layers) where there is some tilting mechanism (e.g., mountain waves, cloud buildup, weather fronts).[1-6]

Based on Eqs. (1) and (2) and the cited literature, the generation of vortices in standing waves is sketched in Fig. 1. In this sketch, a shear layer with a positive tilt angle is shown becoming unstable near the crest of a wave where $\delta\eta$ is at a maximum. The breakdown begins with a folding over of the shear layer and progresses to the formation of vortices that are convected along the downslope of the wave. The resulting array of vortices is called a Kelvin "cat's eyes" pattern. These vortices soon decay and the vorticity is eventually dissipated by viscosity.

Vortex Modeling

The Kelvin cat's eyes pattern is modeled using two-dimensional vortices with horizontal axes. The vortex model consists of a rotational (solid-body) core embedded in an irrotational flow. Each vortex axis is assumed to be perpendicular to the wind vector. The flightpath and vortex geometry used in calculating the wind perturbations during a turbulence encounter are shown in Fig. 2. The distances ℓ and d are the horizontal and vertical separation of the airplane from the vortex; $\Delta\psi$ is the angle between the wind vector and the airplane's flightpath.

The vorticity η is related to vortex strength Γ by the relationships

$$\eta = \frac{\Gamma}{2\pi r_0^2} = \frac{V_0}{r_0}$$

where r_0 is the radius of the solid-body core and V_0 is the velocity tangent to the solid-body core.

The velocity induced at any point on the flightpath outside the solid-body vortex core will have a magnitude $\Gamma/2\pi r$, where r is the distance along a perpendicular from the line vortex and is given as $r = (\ell^2 \cos^2 \Delta\psi + d^2)^{1/2}$. The components of the vortex induced wind are

$$w_{xy} = \frac{\Gamma}{2\pi r_0}\,\frac{r_0 d}{r^2} = V_0\,\frac{r_0 d}{r^2} \tag{3}$$

$$w_z = -\frac{\Gamma}{2\pi r_0}\,\frac{r_0 \ell \cos\Delta\psi}{r^2} = -V_0\,\frac{r_0 \ell \cos\Delta\psi}{r^2} \tag{4}$$

where w_{xy} is in the horizontal direction and w_z is in the vertical direction.

The velocity induced at any point inside the solid-body core will have the magnitude $\Gamma r/2\pi r_0^2$ with components

$$w_{xy} = \frac{\Gamma}{2\pi r_0}\,\frac{d}{r_0} = V_0\,\frac{d}{r_0} \tag{5}$$

$$w = -\frac{\Gamma}{2\pi r_0}\,\frac{\ell \cos\Delta\psi}{r_0} = -V_0\,\frac{\ell \cos\Delta\psi}{r_0} \tag{6}$$

Some typical vortex-induced velocity perturbations that would be experienced by an aircraft passing a single vortex are illustrated in Fig. 3. The aircraft flightpath is assumed to be perpendicular to the line vortex ($\Delta\psi = 0$). For passage directly through the core center ($d/r_0 = 0$) the vertical wind w_z has a maximum value of V_0; for $d/r_0 < 1$ the peak is attenuated; and for $d/r_0 \geq 1$ the peaks in w_z become rounded. The largest peak for the horizontal wind is also V_0, obtained when the flightpath is along the tangent to the cylindrical core ($d/r_0 = 1$).

The velocity perturbation induced by an array of vortices is modeled by superposition of the individual effects. The position of each vortex in the array is determined by matching the modeled winds to the estimated winds during a turbulence encounter. The method for estimating winds from the flight data is considered next.

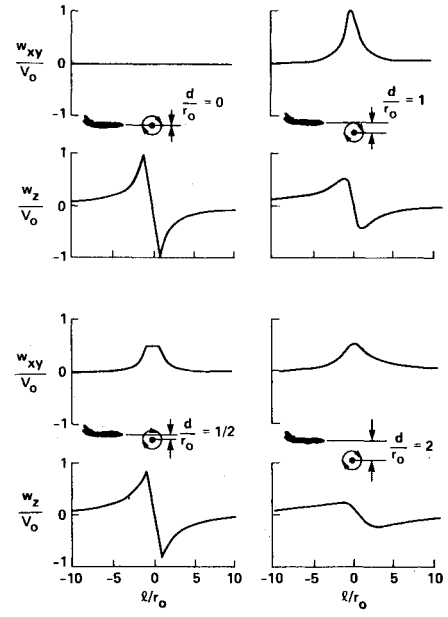

Fig. 3 Vortex-induced velocities encountered at various vertical separations for $\Delta\psi = 0$.

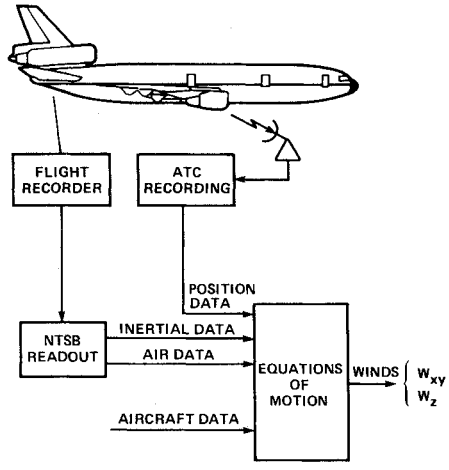

Fig. 4 Estimation of winds from airline operating records.

Wind Estimation

The measurement set available from a digital flight recorder, along with ATC radar data and aircraft performance information, is used in a postflight analysis to estimate winds encountered along a flightpath. A block diagram of the procedure is shown in Fig. 4. The method for wind extraction is based on rigid-body kinematics as presented in Ref. 7 and outlined in this section.

The analysis begins by expressing vehicle accelerations in the Earth frame (here considered to be locally flat, with the x-axis pointing north, the y-axis east, and the z-axis vertical) as

$$\ddot{x} = a_x\cos\theta\cos\psi + a_y(\sin\phi\sin\theta\cos\psi - \cos\phi\sin\psi) + a_z(\cos\phi\sin\theta\cos\psi + \sin\phi\sin\psi)$$

$$\ddot{y} = a_x\cos\theta\sin\psi + a_y(\sin\phi\sin\theta\sin\psi + \cos\phi\cos\psi) + a_z(\cos\phi\sin\theta\sin\psi - \sin\phi\cos\psi)$$

$$\ddot{z} = a_x\sin\theta - (a_y\sin\phi + a_z\cos\phi)\cos\theta - g \qquad (7)$$

where (a_x, a_y, a_z) are onboard measurements of body-axis accelerations and (ϕ, θ, ψ) are onboard measurements of body-axis Euler angles. Integration of differential Eq. (7) provides estimates of inertial velocity $(\dot{x}, \dot{y}, \dot{z})$ and position (x, y, z). A set of initial conditions and bias corrections are determined by matching the calculated x and y time-histories to radar position data and the z time-history to the measured altitude.

The wind velocity is now computed as the difference between the vehicle inertial velocity and its velocity with respect to the air mass. The wind components required for the vortex identification described in the previous section are given by

$$W_{xy} = (W_x^2 + W_y^2)^{1/2}$$

$$W_z = \dot{z} - V_a\sin\gamma_a$$

where

$$W_x = \dot{x} - V_a\cos\psi_a\cos\gamma_a$$

$$W_y = \dot{y} - V_a\sin\psi_a\cos\gamma_a \qquad (8)$$

and the true airspeed V_a is computed from the flight records and the wind-axis Euler angles (γ_a, ψ_a) are found using the identities

$$\sin\gamma_a = \cos\alpha\cos\beta\sin\theta - C\cos\theta$$

$$\tan(\psi_a - \psi) = \frac{\sin\beta\cos\phi - \sin\alpha\cos\beta\sin\phi}{\cos\alpha\cos\beta\cos\theta + C\sin\theta}$$

$$C = \sin\alpha\cos\beta\cos\phi + \sin\beta\sin\phi \qquad (9)$$

where the angles of attack α and sideslip β are determined from the accelerometer measurements, together with a knowledge of the aircraft's aerodynamic characteristics.[7]

Applications

The two encounters with severe turbulence first will be described. The vortex modeling method will then be used to determine the vortex patterns that may account for the estimated winds. Finally, the results will be discussed and compared with previous theory and observations.

Case 1

On April 3, 1981, near Hannibal, Mo., a DC-10 encountered severe turbulence while cruising in an easterly direction at 37,000 ft in the jet stream. As illustrated in Fig. 5a, the encounter occurred shortly after the aircraft passed over a developing line of thunderstorms. The cloud tops were reported to be at about 30,000 ft. Radar echo intensities within the line of thunderstorms reached peak values of 4 (very strong) and 5 (intense).

Figure 5b shows the temperature and wind profiles at Monett, Mo. (upwind side of cloud bank) and at Peoria, Ill. (downwind side of cloud bank). Both soundings were taken approximately 90 min before the encounter. The upwind sounding at Monett indicates a temperature inversion at about 41,000 ft near the tropopause, along with significant windshear layers near the aircraft flight level. The downwind sounding at Peoria indicates a weaker inversion and less severe wind shears.

Because of the direction of the jet stream (240 deg), the air mass containing the turbulence encountered by the airplane would have passed over the more intense cloud buildup to the south of the flightpath (Fig. 5a). A destabilization of the shear layer (i.e., reducing the Richardson number to a critical value) could have been caused by the passage of the jetstream over

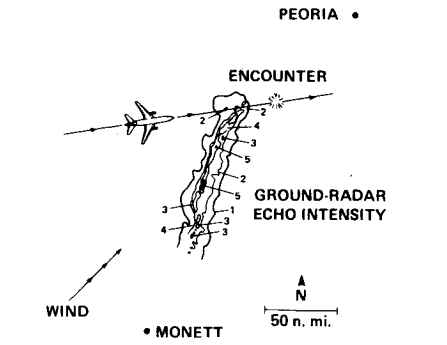

a)Location.

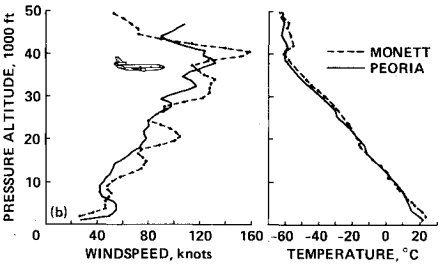

b) Soundings made about 90 min before encounter

Fig. 5 Severe turbulence encounter near Hannibal, Mo., April 3, 1981.

this line of thunderstorms. A stable layer of air, the necessary condition for the generation of vorticity and destabilization by tilting, appears to have existed at Monett at the altitude of the airplane (Fig. 5b; also see Refs. 9 and 10). The Richardson number then would have reached its minimum (critical) value at the tops of the streamlines (Fig. 1) where billowing would occur and vortices with a clockwise rotation would have been convected along the downward sloping streamlines on the downwind side of the clouds.

Figure 6 presents selected time-histories based on information from the flight-data recorder. The estimated horizontal wind W_{xy} and vertical wind W_z are shown, along with the normal acceleration, pitch angle, true airspeed, air temperature, and altitude. The horizontal wind is shown to increase as the aircraft passes over the line of thunderstorms about 2.5 min before the turbulence encounter. The vertical winds in the period of severe turbulence appear as sharp up and down gusts about 5 s apart. The severity of the turbulence is apparent by the wide fluctuations in the normal acceleration from $+1.7$ to -1.0 gs. The associated fluctuations in the measured (barometric) altitude indicate localized variations in the flowfield such as might be expected in the vicinity of vortices. The difference between the measured barometric altitude and the altitude estimated from inertial measurements is illustrated in the bottom plot of Fig. 6.

The vortex model for case 1 is presented in Fig. 7. As shown in the lower graph, the general nature of this model is an array of vortices on the downslope with respect to the prevailing wind and rotating in a clockwise direction. The large spikes in vertical velocity are modeled by passage of the aircraft through the solid body core of two vortices. These spikes provide the more significant evidence about the size and strength of the vortices. For each of the vortices, the modeled values were $r_0 = 600$ ft and $V_0 = 85$ ft/s. The spacing between the two significant vortices is 3500 ft. A comparison of the modeled vertical and horizontal wind perturbations (solid lines) with the estimated winds (dashed lines) shows reasonably good agreement.

Case 2

On July 16, 1982, near Morton, Wyo., a DC-10 airliner encountered severe turbulence while cruising in a westerly

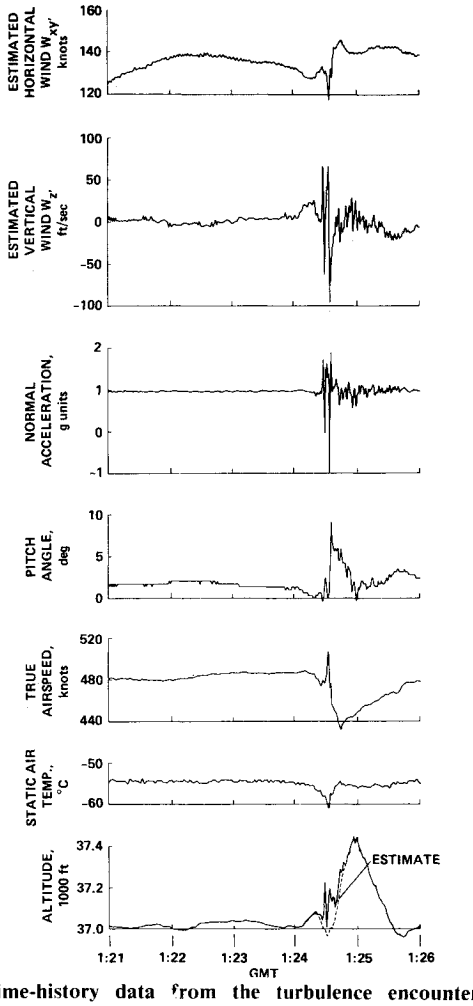

Fig. 6 Time-history data from the turbulence encounter near Hannibal, Mo., April 3, 1981.

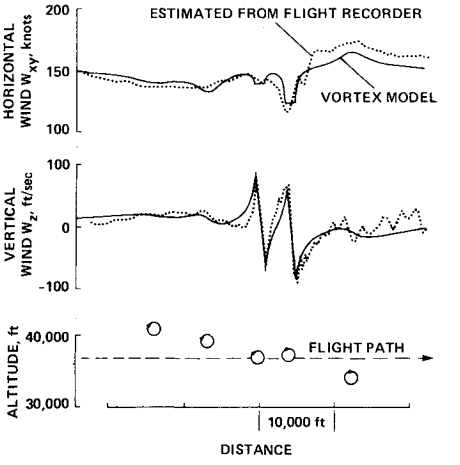

Fig. 7 Vortex array determined from the estimated winds for case 1.

direction at 39,000 ft. As illustrated in Fig. 8a, this encounter occurred as the aircraft was approaching the Wind River Mountain range. The direction of the prevailing wind was into the path of the aircraft and perpendicular to the mountain range.

Figure 8b shows the wind and temperature profiles at Salt Lake City (upwind of the mountains). Figure 8c shows the wind and temperature profiles at Lander, Wyo. (downwind of the mountains). These soundings were made at 1200 GMT and 2400 GMT. The encounter occurred at about 1800 GMT, at a time between the two soundings. A temperature inversion at the tropopause is indicated in the 1200 GMT sounding at

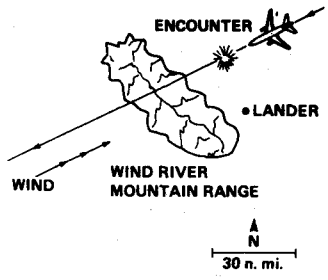

a) Location.

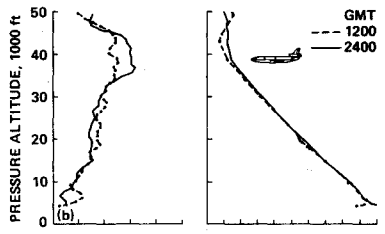

b) Soundings at Salt Lake City, Utah.

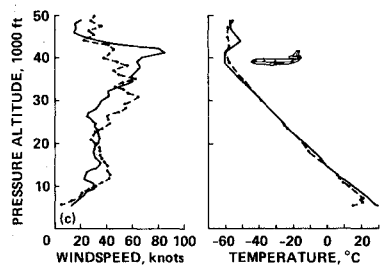

c) Soundings at Lander, Wyo.

Fig. 8 Severe turbulence encounter near Morton, Wyo., July 16, 1982.

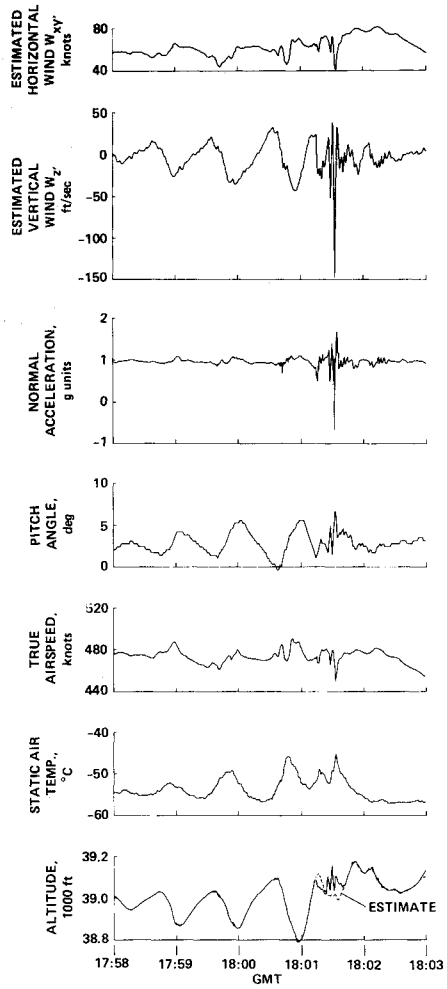

Fig. 9 Time-history data from the turbulence encounter near Morton, Wyo., July 16, 1982.

the upwind station and later in the 2400 GMT sounding at the downwind station. As compared with the upwind sounding at Salt Lake City, the downwind soundings at Lander indicate strong wind-shear layers. In particular, the 1200 GMT sounding at Lander indicates several layers of wind shear that are indicative of mountain wave activity.

The pilot reported that mountain waves became apparent about 50 mi. downwind of the Wind River range before the severe turbulence encounter. Portions of this mountain wave and the subsequent turbulence encounter are illustrated by the time-histories presented in Fig. 9. The time-histories show the mountain-wave acitivity as sinusoidal fluctuations with a period of from 55 to 60 s. As the aircraft approached the mountains, the amplitude of these fluctuations increased. The peak-to-peak excursions in vertical velocity reached about 60 ft/s, and the excursions in the air temperature reached about 10°C, indicating standing waves of fairly large amplitudes. In the period of severe turbulence, the vertical winds appear as sharp up and down gusts about four s apart. The severity of the turbulence encounter is apparent by the fluctuations in the normal acceleration from +1.6 to −0.6 *g*s. The associated fluctuations in the measured (barometric) altitude indicate localized variations in the flowfield.

The vortex model for case 2 is presented in Fig. 10. The general nature of this model is an array of vortices near the aircraft flightpath. For each of the vortices, the modeled values were $r_0 = 450$ ft and $V_0 = 70$ ft/s with spacings of about 3200 ft. A comparison of the modeled wind perturbations with the estimated winds shows some agreement, but not as good as that shown previously for case 1. The problem in modeling the winds in case 2 appears to be the presence of strong mountain wave activity which influences the short-period wind pattern. This was not the situation in case 1, in which the wave activity was fairly mild in comparison.

Discussion

There are certain similarities in the two CAT encounters analyzed in this paper. Each occurred during level flight near the tropopause where the existence of a statically stable shear layer was indicated. Each case involved a tilting mechanism that could have triggered Kelvin-Helmholtz instability. And finally, each encounter consisted of a short series of sudden, violent disturbances with definite periodicity.

The results of this paper are in general agreement with a variety of other evidence based on theory, ground-based observations, and aircraft flight tests as follows:

1) The relationship between the spacings of the vortices and their core diameter is in general agreement with previous evidence. Scorer[6] calculated that the ratio of spacing to core diameter would be of the order of 2.7. For the two cases discussed in this paper, the ratio of spacing to core diameter ranged from about 2.9 to 3.5.

2) Previous observations of vortices near the tropopause have been made by high-power, ground-based radar.[3,11] These radar observations indicated vortex core diameters of the order of 900 to over 1500 ft. The vortices in this study had core diameters of the order of 900 to 1200 ft which are consistent with these ground-based observations.

3) The records obtained from a large variety of airline operations[12,13] indicate that there have been instances when vertical wind gusts have reached values of the order of 50 to 80 ft/s. In both cases discussed here, the maximum value of

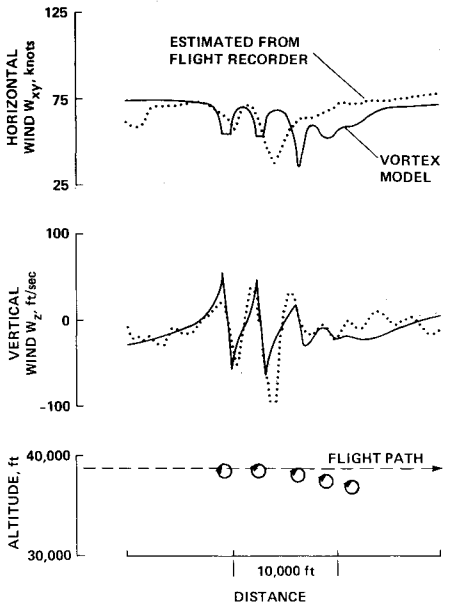

Fig. 10 Vortex array determined from the estimated winds for Case 2.

vortex-induced velocities were of the same order of magnitude.

4) Recent flight studies[14] using a microwave radiometer indicate that inversion layers at the tropopause are most frequently associated with severe CAT. In both of the cases discussed here, there were tropopause temperature inversions indicated near the aircraft altitudes.

Conclusions

Some results have been presented that illustrate the way in which the nature and cause of CAT can be analyzed using available flight records of airline encounters with severe turbulence. Two case studies were considered in which destabilization of shear layers and the generation of vortices appeared to have been caused by tilting, in one case by cloud buildup in the lower atmosphere, and in the other by mountain lee waves. Vortex models were used to reproduce analytically the array of vortices producing wind perturbations similar to those experienced by the aircraft. Vortex models appear to be promising aids in achieving a better understanding of the periodic, deterministic nature of the severe turbulence. The results obtained using vortex modeling also appear consistent with previous ideas about severe CAT that were based on theory and observations.

References

[1] Ludlam, F. H., "Characteristics of Billow Clouds and Their Relation to Clear Air Turbulence," *Quarterly Journal of the Royal Meteorological Society*, Vol. 92, 1967, pp. 419-435.

[2] Clark, J. W., Stoeffler, R. C., and Vogt, P. G., "Research on Instabilities in Atmospheric Flow Systems Associated with Clear Air Turbulence," NASA CR-1604, 1970.

[3] Browning, K. A., Watkins, C. D., Starr, J. R., and McPherson, A., "Simultaneous Measurements of Clear Air Turbulence at the Tropopause by High-Power Radar and Instrumented Aircraft," *Nature*, Vol. 228, Dec. 12, 1970, pp. 1065-1067.

[4] Gossard, E. E. and Hooke, W. H., *Waves in the Atmosphere*, Elsevier Scientific Publishing Co., New York, 1975.

[5] Hopkins, R. H., "Forecasting Techniques of Clear-Air Turbulence Including That Associated with Mountain Waves," World Meteorolgical Organization Technical Note No. 155, 1976.

[6] Scorer, R. S., *Environmental Aerodynamics*, Wiley, New York, 1978.

[7] Parks, E. K., Bach, R. E., Jr., and Wingrove, R. C., "Analysis of the Nature and Cause of Turbulence Upset Using Airline Flight Records," *Symposium of the Society of Flight Test Engineers*, New York, N. Y., Sept. 1982.

[8] Taylor, L. W. and McLaughlin, M. D., "A Modified Newton-Raphson Analysis of Flight Measurements of the Trailing Vortices of a Heavy Jet Transport," NASA TN D-7404, Aug. 1974.

[9] Keller, J. L., "Performance of a Quantitative Jet Stream Turbulence Forecasting Technique: The Specific CAT Risk (SCATR) Index," AIAA Paper 84-0271, Reno, Nev., Jan. 1984.

[10] Keller, T. L., Ehernberger, L. J., and Wurtele, M. G., "Numerical Simulation of the Atmosphere During a CAT Encounter," *Proceedings of the Ninth Conference on Aerospace and Aeronautical Meterology*, American Meteorological Society, Boston, June 1983, pp. 316-319.

[11] Hardy, K. R., "Studies of the Clear Atmosphere Using High Power Radar," *Remote Sensing of the Troposphere*, National Oceanic and Atmospheric Administration, Boulder, Colo., 1972, chap. 14.

[12] Pratt, K. G. and Walker, W. G., "A Revised Gust-Load Formula and a Reevaluation of V-G Data Taken on Civil Transport Airplanes from 1933 to 1950," NACA Report 1206, 1954.

[13] Zalovick, J. A., Jewel, J. W., and Morris, G. J., "Comparison of VGH Data from Wide-Body and Narrow-Body Long-Haul Turbine-Powered Transports," NASA TN D-8481, 1977.

[14] Gary, B., "Clear Air Turbulence Avoidance Using an Airborne Microwave Radiometer," AIAA Paper 84-0273, Reno, Nev., Jan. 1984.